

Effect of Wall Properties Without/with Magnetic Field on NanoBingham Fluid Flows

Muhammad Magdy^{1,*}, Islam Eldesoky^{1,2}, Ramzy Abumandour¹

¹Basic Engineering Sciences Department, Faculty of Engineering, Menoufia University, Shebin El-Kom, Egypt

²Elmenofia Higher Institute of Engineering and Technology, El-Menofia, Egypt

Email address:

moh.magdy@sh-eng.menoufia.edu.eg (Muhammad Magdy)

*Corresponding author

To cite this article:

Muhammad Magdy, Islam Eldesoky, Ramzy Abumandour. (2024). Effect of Wall Properties Without/with Magnetic Field on NanoBingham Fluid Flows. *Fluid Mechanics*, 9(1), 1-13. <https://doi.org/10.11648/j.fm.20240901.11>

Received: October 25, 2023; **Accepted:** November 13, 2023; **Published:** January 18, 2024

Abstract: In this study the steady flow of nano Bingham plastic fluid with wall properties under the effect of an external magnetic field and the peristaltic motion has been analyzed. Flow of nano Bingham plastic fluid is considered as non-Newtonian fluid. The nanofluid interaction theory is investigated by considering equations of motion of both the nanofluid and flexible boundary. The governing equations are solved analytically under the long wavelength and low Reynolds number approximation. Analytical forms estimates are obtained for the velocity profile, volumetric flow rate, pressure gradient and wall shear stress. The study shows that for a given yield stress, both the nanofluid velocity reduce, as the strength of the magnetic field is increased, but the velocity of the nanofluid increase with the rise in permeability parameter (k). The effect of the wall tension, wall damping and wall elastic on the velocity has been studied. With damping, the velocity increases. Through the analysis, we obtained that the yield stress increases the velocity. The effects of amplitude ratio δ on the complicated behavior of streamlines have been discussed. With increasing the magnetic field and the yield stress, the streamlines are strongly crowded. The pressure difference along the artery affects the tension in the wall of artery, the damping of the wall and the amplitude ratio, where the wall tension or the amplitude ratio increases, pressure difference increases. The study will be useful for dealing with problems related to blood flow in arteries in a pathological state, where the lumen of the artery has turned into a porous structure due to formation of blood clots.

Keywords: Peristaltic Motion, Nanofluids, Nano-Bingham, Wall Properties, MHD, Porous Medium

1. Introduction

Peristaltic pumping is the theory of the fluid transport in a flexible tube due to a progressive wave of contraction or expansion from a lower pressure region to higher pressure region. There are many applications on this motion, like urine transport from kidney to bladder through the ureter, the movement of spermatozoa in the ducts afferents of the male reproductive tract and the ovum in the female fallopian tube, transport of lymph in the lymphatic vessels, vasomotor of small blood vessels such as arterioles, the locomotion of some worms, venules and capillaries involves the peristaltic motion and movement of chyme in the gastrointestinal tract.

Nanofluids, a revolutionary class of fluids, are colloidal suspensions of nanoparticles in base fluids. These

nanoparticles typically have sizes ranging from 1 to 100 nanometers and are dispersed uniformly throughout the base fluid. Nanofluids exhibit enhanced thermal, electrical, and optical properties compared to traditional fluids, making them highly sought after for various applications. One of the significant applications of nanofluids lies in heat transfer systems. Due to their exceptional thermal conductivity, nanofluids are used to improve the efficiency and performance of heat exchangers, cooling systems, and electronics cooling. Additionally, nanofluids find utility in solar energy systems, automotive industries, and advanced manufacturing processes where their exceptional properties enable enhanced energy transfer, lubrication, and heat dissipation. The versatility and potential of nanofluids continue to expand, paving the way for innovative applications in diverse fields.

Kalbande et al. [1] investigated the global mathematical correlations for heat pipe and nanofluid based thermal energy storage system. This work presents the development of a mathematical model for a nanofluid-based thermal energy storage (TES) system. The main objective of the study is to establish global correlations among various performance parameters of the TES system. The TES system considered in this research employs Al₂O₃/Soybean oil as the heat transfer fluid (HTF), and heat pipes are integrated to enhance heat transfer between the HTF and the phase change material.

Analysis of the performance of the novel heat-pipe-assisted thermal storage system with parabolic trough solar collector and nanofluid was studied by Mohan et al. [2]. The thermal energy storage system is nanofluid (Al₂O₃/soybean oil) based and the eutectic mixture of KNO₃ and NaNO₃ (nitrate salt) in the molar ratio of 40:60 has been used as phase change material to store the heat energy. The system is based on the natural circulation of heat transfer fluid (thermo-syphon) and the receiver to arrest the solar radiation is parabolic trough solar collector using an evacuated tube. It is observed that, for the same charging cycle time and same climatic conditions, the compared value of specific heat storage capacity is 67% higher as compared to the average value of other considered systems.

Kalbande, and Walke [3] investigated the oil-and aluminum-based thermal storage system using flat plate solar collector. The oil- and aluminum-based energy storage system is used for experimentation and having same storage potential and to store the energy in storage contain phase change material which have melting temperature of 210–220 °C. Energy collected by solar collector heated the fluid contained in receiver tube and carry the energy to storage space. The self-circulation unit is introducing between storage and solar collector which contain soybean oil as a heat transfer fluid. The main aim of the concept is to store energy during day and utilized it in nighttime for cooking purpose.

Kriplani et al. [4] presented advancements in thermal energy storage system by applications of Nanofluid based solar collector. It is observed that the thermal energy storage system (TES), using solar collector, is a useful device for storing sensible and latent heat in a unit volume. The nanoparticles find the use in various industrial applications because of its properties, such as thermal, mechanical, optical, and electrical. The parabolic solar collector using nanofluid is still a challenge. This work showed an exhaustive review of thermal storage system using nanofluid based solar collector and a scope of using nanofluid based solar collector for performance enhancement.

The performance enhancement of thermal energy storage systems using nanofluid have been showed by Sharma et al. [5]. Due to upsurge in the energy demand the usage of fossil fuel has increased dramatically. To find the substitute of fossil fuel is one of the vital issues throughout the world. The combustion of fossil fuel has severe effect not only on environment but also on human health. The most common way of storing energy in the form of latent heat is carried out

by using phase change materials (PCM). The common issues with traditional PCM are their poor thermal conductivity which can be enhanced by using nanoparticles. The charging rate and efficiency of TES can be boosted by using nanofluid.

In Bingham plastic fluids, the ratio between the applied stress and the yield stress varies linearly with shear rate. These fluids are considered as non-Newtonian behavior. In the absence of a velocity gradient, they bear the potential to transmit shear stress even. Thus, there is a linear relationship between shear stress and strain for Bingham plastic fluids. At a low stress level, the motion of Bingham plastic fluids is very similar to that of a rigid body, but when the stress level is high, they flow like a viscous fluid. It has been found that Bingham liquids possess thicker coating in comparison to the case of Newtonian fluids. Drilling mud, printing ink, molten liquid, clay, toothpaste paint, foams, and food articles like margarine, mayonnaise, molten chocolate, yoghurts, and ketchup are some typical examples of Bingham plastics. Since Bingham fluids are transformed to solids when the applied shear stress is less than the yield stress, it is apparent that Bingham fluids behave like a solid medium in the core layer. That means, a solid plug moves within the flow.

Viscoplastic models that include Bingham plastic model, Herschel-Bulkley model and Casson model have been analyzed by Mitsoulis [6]. He showed the entry and exit flows from dies, flows around spheres and cylinders, as well as squeeze flows. A two-dimensional study on creeping flow of a Bingham plastic fluid through a cylinder was investigated numerically by Nirmalkar et al. [7], who reported that in the limit of plastic flow, drag approaches a constant value. Bahaduri et al. [8] developed a simple predictive tool that can be used to easily predict the boundaries of the plug of Bingham plastic fluids for laminar flow through annulus. Sayad-Ahmed et al. [9] used a numerical method to examine thermally laminar heat transfer based on the fully developed velocity for Bingham fluids in the entrance region of a circular duct. A review of different studies on the yield stress of blood has been produced by Paicart et al. [10]. The Bingham plastic characteristics of blood flow through a stenosed artery were recently discussed by Yadav and Kumar [11]. Singh and Singha [12] considered the fully developed one dimensional Bingham plastic flow of blood through a small artery having multiple stenosed and poststenotic dilation. De-Chant [13] used regular perturbation method for the oscillatory flow of a Bingham plastic fluid, where there is a relationship between the velocity field and dimensionless flow rate. This study was present blood flow in arteries in a pathological state and his solution develops useful analytical models that bear the potential to support experimental and computational studies on arterial blood flow.

Non-Newtonian fluids are the actual state of the fluids, particularly for the complexity of blood and its flow in normal/diseased arteries, they have used different non-Newtonian models, like, Casson model, couple stress fluid model, power law fluid model, micropolar fluid model, viscoelastic fluid model and Herschel-Bulkley fluid model.

The objective of the problem study leads us to select a particular model. Some of their studies concerned with arterial blood flow in the normal physiological state, while some others are concerned with blood flow in arteries under pathological conditions. Misra et al. [14] studied some of the hemorheological states.

Peristaltic motion of blood in the microcirculatory system was studied by Misra and Maiti [15], in which the non-Newtonian behavior of blood has been modeled as a Herschel-Bulkley fluid and the model has been treated to be different cross section. It is observed that the Herschel-Bulkley fluid model is more general than most other non-Newtonian models and that the results for a fluid represented by the Bingham plastic fluid model can be derived from those of any study conducted with consideration of blood as a Herschel-Bulkley fluid.

The effect of thermal radiation on the magnetohydrodynamic flow of blood and heat transfer in a permeable capillary in stretching motion has been presented by Misra and Sinha [16]. Where, the lumen of the capillary has been designed as a porous structure due to some arterial disease. The results obtained based on the study have an important bearing on the therapeutic procedure of electromagnetic hyperthermia, particularly in understanding/regulating blood flow and heat transfer in capillaries.

The effect of swirling flow and heat transfer analysis on MHD fluid subject to partial slip and temperature jump conditions analyzed by Kumar et al [17]. They examine the problem of swirling flow for the Reiner–Rivlin liquid where the surface of rotating disk admits the Navier's velocity slip condition within the environment of magnetic field. The temperature jump condition because of imperfect liquid–solid energy accommodation is also considered. Amit et al. [18] studied the unsteady mixed convective flow of hybrid nanofluid past a rotating sphere with heat generation/absorption: an impact of shape factor. This study aims to examine the flow of unsteady mixed convective hybrid nanofluid over a rotating sphere with heat generation/absorption. The hybrid nanofluid contains different shapes of nanoparticles (copper [Cu] and aluminum oxide [Al₂O₃]) in the base fluid (water [H₂O]).

Eldabe et al. [19] studied the effects of the pressure work and Hall currents in the MHD peristaltic flow of Bingham–Papanastasiou nanofluid through porous media. The influences of the Hall currents on the motion of a non-Newtonian nanofluid with heat and mass transfer inside a vertical symmetric channel have been analyzed. The fluid conforms to the Bingham–Papanastasiou model. Concerning the assumptions of the long wavelength and low Reynolds number, the resulting equations are solved by utilising the homotopy perturbation method (HPM). It is found that as the Bingham factor is increased, both axial velocity and temperature are also increased. When the pressure work and Hall current coefficients increase, both temperature and pressure gradient decrease. The Brownian motion and thermophoresis parameters have different influence on the nanoparticle concentration distribution. Furthermore, it is

shown that the heat transfer coefficient is a decreasing function in both Hall and thermal radiation parameters.

Sultan et al. [20] Investigated of biological mechanisms during flow of nano-Bingham–Papanastasiou fluid through a diseased curved artery. This study aims to explore the biological flow mechanisms in a diseased curved artery during the flow of nano-Bingham–Papanastasiou fluid. The occurrence of stenosis and aneurysm is common in the arterial system, caused by narrowing or dilation of arteries owing to the development of abnormal tissues such as atherosclerotic plaques. The growth of these cells into the lumen of the artery disturbs the flow through the artery. For the treatments of hematological diseases and manufacturing nanoscale biomedical devices, nanofluids are very effective and gaining a lot of attention. In this study, Buongiorno's nanofluid model is used for nanoscale effects and Bingham–Papanastasiou fluid is employed to study the hemodynamic rheology.

The Dufour and Soret impacts on magnetohydrodynamic Carreau nanoliquid past a nonlinearly stretching sheet are analyzed by Basha et al. [21]. Variations in viscosity, heat conductivity, and convective boundary conditions are considered. Suitable similarity conversions are utilized to design the governing equations nondimensional. It is observed that when the Dufour number increases, the temperature distributions get narrower. However, with increasing Soret number, the concentration distribution has the opposite effect. One of the important outcomes of the study is that by increasing the Weissenberg number for shear-thinning fluids, one can improve the velocity field.

The motion of hybrid nanosuspension across a wedge under the effect of convectively warmed boundary conditions is analyzed for nanoparticles of different shapes by Amit et al. [22]. To analyze the nanomaterial, the flow model is developed, and it makes use of the Buongiorno nanofluid model to do so. Both the basic slip mechanisms and the effective properties of the hybrid nanoliquid are accounted for the flow model. The swirling flow problem for the nanoliquid over a radially stretchable rotating disk with the consideration of nonlinear mixed convection and chemical reaction defined by Arrhenius model studied by Kumar et al. [23]. The surface of the stretchable rotating disk concedes with the Navier's velocity slip condition. The temperature jump condition due to imperfect liquid–solid energy interaction is also considered.

Ray et al. [24] illustrate incompressible convective flow of kinetic theory-based Eyring–Powell fluid conveying nano-sized particle from a vertical plate with convective boundary condition and distribution of nanoparticles fraction over its surface. Cattaneo–Christov model is imposed to scrutinize the heat transfer analysis. A revised Buongiorno model is adopted, which considers zero nanoparticle flux at the wall surface and simulates physically more viable scenarios for nanoparticle distribution. Free convection flow of Jeffrey nanofluid past a vertical plate with sinusoidal variations of surface temperature and species concentration is presented by Vasu et al. [25]. The study of heat transfer and nanofluid

transport has been done by employing Cattaneo–Christov heat flux model and Buongiorno model.

The impact of the magnetic dipole for the flow of non-Newtonian Williamson nanoliquid by considering the thermal radiation and chemical reaction defined by the Arrhenius model is introduced by Kumar *et al.* [26]. The flow model is established by incorporating the well-known Buongiorno's nanofluid model, and as a result, Brownian motion and thermophoretic diffusion are assimilated in mathematical modeling. Ray *et al.* [27] analyzed an incompressible flow of a non-Newtonian Spriggs fluid over an unsteady oscillating plate is investigated using the Homotopy Analysis Method (HAM). Two dimensional and steady heat transfer over a cylinder in a porous medium with suspending nanoparticles is investigated by Ray *et al.* [28]. Buongiorno model is adopted for nanofluid transport on a free convection flow taking the slip mechanism of Brownian motion and thermophoresis into account.

Darcy and Brinkman models are important in describing the flow of various biological fluids with porous media. It has been found that models for flow through porous media are widely applicable in the simulation of blood flow in tumors and in modeling blood flow when fatty plaques of cholesterol and artery-clogging clots are formed in the lumen of an artery. Eldesoky, [29], studied the Slip effects on the unsteady MHD pulsatile flow through a porous medium in an artery under the effect of body acceleration. Ravi Kumar, [30], analyzed the analysis of heat Transfer on MHD peristaltic blood flow with porous medium through coaxial vertical tapered asymmetric channel with radiation.

Diagnose cardiovascular diseases require the interaction of a magnetic field with blood flow. Magnetic fields are used to develop devices for cell separation, targeted transport of drug using magnetic particles as drug carriers, reduction of bleeding during surgeries and provocation of occlusion of feeding vessels of cancerous tumors and development of magnetic tracers. For this reason, studies of flow properties of human blood as well as deformation of blood vessels subject to an applied external magnetic field were conducted by several researchers [31–37].

Radial momentum

$$\rho_{nf} \left[\frac{\partial w'}{\partial t'} + u' \frac{\partial w'}{\partial r'} + w' \frac{\partial w'}{\partial z'} \right] = -\frac{\partial p'}{\partial z'} - \frac{\mu_{nf}}{r'} \left(\frac{\partial(r' \tau')}{\partial r'} \right) - \sigma \beta_o^2 w' - \frac{\mu}{k} w', \quad [38] \quad (3)$$

$$\rho_{nf} \left[\frac{\partial u'}{\partial t'} + u' \frac{\partial u'}{\partial r'} + w' \frac{\partial u'}{\partial z'} \right] = -\frac{\partial p'}{\partial r'} + \mu_{nf} \left(\frac{\partial^2 u'}{\partial r'^2} + \frac{1}{r'} \frac{\partial u'}{\partial r'} - \frac{u'}{r'^2} + \frac{\partial^2 u'}{\partial z'^2} \right) \quad [38] \quad (4)$$

where u' and w' are the velocity components, μ_{nf} is the coefficient of dynamic viscosity of nanofluid, K_{nf} is the thermal conductivity of nanofluid.

$$\tau' = \tau'_y - \mu \frac{\partial w'}{\partial r'}, \quad \text{at } \tau' \geq \tau'_y, \quad [39] \quad (5)$$

2. Formulation of the Problem

Consider an incompressible non-Newtonian nanofluid (Bingham fluid) of viscosity μ_{nf} and density ρ_{nf} flowing through a composite sinusoidal artery of finite length L . Assume (r', z') be the coordinates of a material point in the cylindrical polar coordinate system where z' -axis is taken along the axis of artery, while r' is the radial direction, respectively. $r' = 0$ is taken as the axis of symmetry of the tube. The geometry of the arterial wall with sinusoidal wave is written mathematically as:

$$H'(z', t') = R_o + \delta' \sin \left(\frac{2\pi}{\lambda} (z' - u_o t') \right) \quad [38] \quad (1)$$

Geometry of Problem

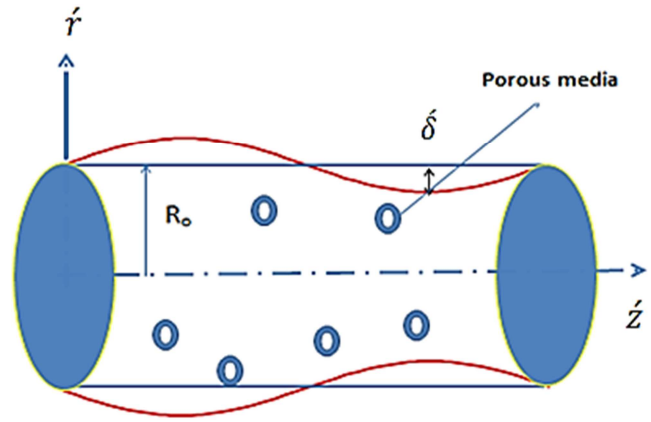


Figure 1. Geometry of Problem.

Mass equation

$$\frac{1}{r'} \frac{\partial}{\partial r'} (r' u') + \frac{\partial}{\partial z'} (w') = 0 \quad (2)$$

Axial momentum

$$-\frac{\partial w'}{\partial r'} = 0, \quad \text{at } \tau' \leq \tau'_y, \quad (6)$$

The boundary conditions that must be satisfied by the nanofluid on the wall and the catheter are the slip conditions suggested by Kwang and Fang [40]. These can be written as:

$$w' = 0, \quad \text{at } r' = h(z'), \quad (7)$$

$$\frac{\partial w'}{\partial r'} = 0, \text{ at } r' = 0, \quad (8) \quad r = \frac{r'}{R_o}, \quad w = \frac{w'}{u_o}, \quad \zeta^2 = \frac{\rho_f \omega R_o^2}{\mu_f}, \quad t = \omega t', \quad \tau = \frac{\tau'}{\tau_c}, \quad \tau_y = \frac{\tau'_y}{\tau_c},$$

$$\frac{\partial p'}{\partial z'} = \frac{dp'}{dz'} = \frac{\partial}{\partial z'} \left(-m_1 \frac{\partial^2 \eta'}{\partial z'^2} + m_2 \frac{\partial^2 \eta'}{\partial t'^2} + m_3 \frac{\partial \eta'}{\partial t'} \right) [41] \quad (9) \quad \tau_c = \frac{\mu_f u_o}{R_o}, \quad u_o = -\frac{p_o R_o^2}{2\mu_f}, \quad \varepsilon = \frac{R_o}{L_o}, \quad Ha = \sqrt{\frac{\sigma_f}{\mu_f}} \beta_o R_o,$$

m_1 tension in the membrane

m_2 mass per unit area of the membrane

m_3 coefficient of viscous damping force of the membrane

$$\eta'(z', t') = \delta' \sin \left(\frac{2\pi}{\lambda} (z' - u_o t') \right)$$

$$k = \frac{k'}{R_o}, \quad \delta = \frac{\delta'}{R_o}, \quad Re = \frac{\rho_f u_o L_o}{\mu_f}$$

The dimensionless parameters indicated as k is the permeability parameter, u_o is wave velocity, ε is wave number and δ is amplitude ratio.

Substituting the dimensionless parameters into the governing equations (2 - 9), yields the following equations:

Introducing the following dimensionless variables $z = \frac{z'}{\lambda}$, $\frac{1}{r} \frac{\partial}{\partial r} (ru) + \frac{\partial}{\partial z} (w) = 0$, (10)

$$\frac{\rho_{nf} \omega R_o^2}{\mu_f} \left[\frac{\partial w}{\partial t} \right] = \frac{p_o R_o^2}{\mu_f u_o} \frac{\partial p}{\partial z} - \frac{\mu_{nf} \tau_c R_o^2}{u_o R_o \mu_f r} \left(\frac{\partial(r\tau)}{\partial r} \right) - Ha^2 w - \frac{1}{k} w \quad (11)$$

$$\frac{\rho_{nf}}{\rho_f} \zeta^2 \varepsilon^3 \delta \left[\varepsilon \delta u \frac{\partial u}{\partial r} + w \frac{\partial u}{\partial z} \right] = -\frac{\partial p}{\partial r} + \frac{\mu_{nf}}{\mu_f} \left(\delta \frac{\partial^2 u}{\partial r^2} + \frac{\delta}{r} \frac{\partial u}{\partial r} - \delta \frac{u}{r^2} + \varepsilon \frac{\partial^2 u}{\partial z^2} \right) \quad (12)$$

Using the dimensionless parameters also in the amplitude equation leads to:

reduced to:

Reduced radial momentum equation

$$h = 1 + \eta = 1 + \delta \sin(2\pi(z - t))$$

$$\frac{\partial p}{\partial r} = 0 \text{ thus } \frac{dp}{dz} = \frac{\partial p}{\partial z}, \quad (13)$$

Non dimensionalization and Solution Method

Using the long wavelength approximation ($\delta \ll 1, \varepsilon \approx O(1)$) as considered in Shapiro et al. [42], the equations describing the flow in the stenosis frame can be

Reduced axial momentum equation

$$\left[\frac{\partial^2 w}{\partial r^2} + \frac{1}{r} \frac{\partial w}{\partial r} \right] - (1 - \phi)^{2.5} \left(Ha^2 + \frac{1}{k} \right) w = \frac{\tau_y}{r} + (1 - \phi)^{2.5} \frac{dp}{dz}, \quad r_p \leq r \leq h(z), \quad (14)$$

$$w_p = w, \quad 0 \leq r \leq r_p$$

With velocity boundary conditions as:

$$w = 0 \text{ at } r = h(z), \quad (15)$$

$$\frac{\partial w}{\partial r} = 0 \text{ at } r = r_p, \quad (16)$$

The dimensionless parameters in the previous equations are: Ha = Hartman number, $(1/k)$ is porosity, τ_y is yield stress.

The expression for the velocity profiles w can be obtained as the solution of the equations (14), subjected to the boundary conditions (15) and (16):

$$w = C_1 b r_1 + C_2 b r_2 + \tau_y r - \frac{\frac{dp}{dz}}{\left(Ha^2 + \frac{1}{k} \right)}, \quad \text{for } r_p \leq r \leq h(z), \quad (17)$$

$$w_p = w, \quad \text{for } 0 \leq r \leq r_p$$

The stream function can be obtained from the relation of the velocity as:

$$w = \frac{1}{r} \frac{\partial \psi}{\partial r}$$

$$\psi(z, r) = \int r w(z, r) dr \quad (18)$$

where C_1, C_2 are

$$C_1 = \frac{q_4 \left(-\tau_y h + \frac{\frac{dp}{dz}}{\left(Ha^2 + \frac{1}{k} \right)} \right) - (-\tau_y b h_2)}{(b h_1 q_4) - (b h_2 q_3)}, \quad C_2 = \frac{(-\tau_y b h_1) - q_3 \left(-\tau_y h + \frac{\frac{dp}{dz}}{\left(Ha^2 + \frac{1}{k} \right)} \right)}{(b h_1 q_4) - (b h_2 q_3)}$$

From which,

$$b r_1 = I_0(\sqrt{B} r) = 1 + \frac{B r^2}{4} + \frac{B^2 r^4}{64},$$

$$b r_2 = K_0(\sqrt{B} r) = -\ln\left(\frac{\sqrt{B} \cdot r}{2}\right) - \frac{B r^2 \ln\left(\frac{\sqrt{B} \cdot r}{2}\right)}{4} + \frac{(2-2\gamma) B r^2}{8},$$

$$b h_1 = I_0(\sqrt{B} h), b h_2 = K_0(\sqrt{B} h), b r_{p1} = I_0(\sqrt{B} r_p), b r_{p2} = K_0(\sqrt{B} r_p),$$

$$q_1 = \frac{\partial b h_1}{\partial h}, q_2 = \frac{\partial b h_2}{\partial h}, q_3 = \frac{\partial b r_{p1}}{\partial r_p}, q_4 = \frac{\partial b r_{p2}}{\partial r_p},$$

I_0 is zero order modified Bessel function of the first kind.

K_0 is zero order modified Bessel function of the second kind.

We can obtain the pressure difference from the compliant wall as:

$$\frac{dp}{dz} = \frac{\partial p}{\partial z} = p(z) = \left(-\frac{A_1}{\text{Re}^2} \frac{\partial^3 \eta}{\partial z^3} + A_2 \frac{\partial^3 \eta}{\partial t^2 \partial z} + \frac{A_3}{\text{Re}} \frac{\partial^2 \eta}{\partial t \partial z} \right)$$

$$\Delta p = - \int_0^l \frac{dp}{dz} dz \quad (19)$$

Validation of the Present Model with Misra Model

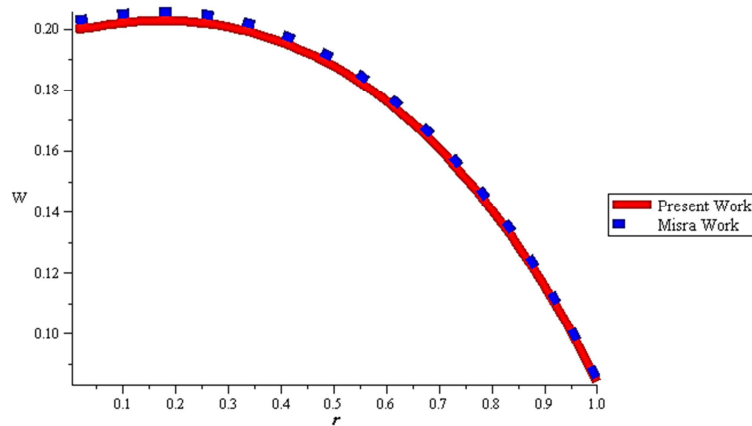


Figure 2. Velocity profiles validation at ($A_1=1, A_2=0.01, A_3=1, Ha=2, \delta=0.2, \tau_y=0.05, k=0.5, r_p=0.01, \varphi=0.2$).

3. Results and Discussions

3.1. Problem Validation

Equation (17) represents the same formula of Misra and Adhikary [39] when ignoring the effect of peristaltic motion, nanoparticles concentration, wall properties on the flow behavior, as shown in the following figure.

3.2. Analysis and Discussion

In this analysis the magnetic field and wall properties effects on the peristalsis of a non-Newtonian fluid in pipe have been investigated. The non-dimensional velocity streamlines and pressure difference of the nanofluid at different values of parameters such as the nanoparticle concentration, ϕ and the amplitude ratio, δ are considered. The parameter values are chosen as: R_0 (tube radius) = 1.25 cm; $\phi = 0, 0.02, 0.04$; $\delta = 0.1, 0.2$, and 0.3 .

For $0 \leq r \leq r_p$ the magnitude of the velocity is constant with the radius of the plug (r_p). Figure 3. represents the

Velocity profiles with different nanoparticles concentration

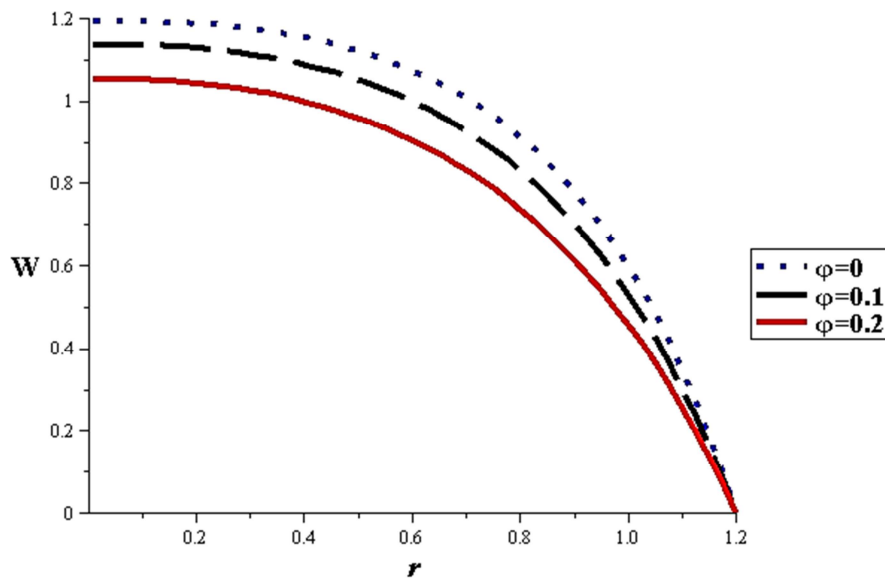


Figure 3. Velocity profiles with different nanoparticles concentration at ($A_1=1, A_2=0.01, A_3=1, Ha=1.5, \delta=0.2, \tau_y=0.05, k=0.1, r_p=0.01$).

Velocity profiles with different amplitude ratio

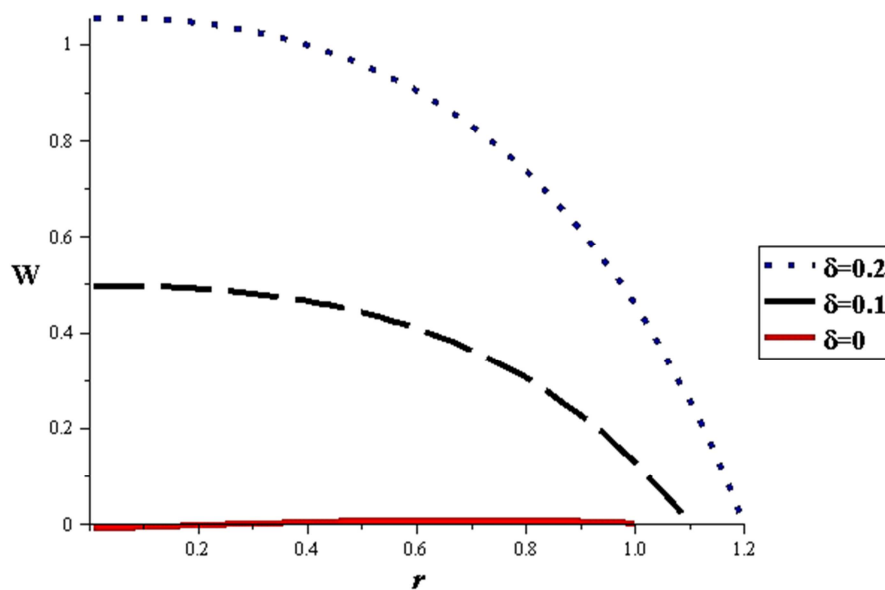


Figure 4. Velocity profiles with different amplitude ratio at ($A_1=1, A_2=0.01, A_3=1, Ha=1.5, \tau_y=0.05, \phi=0.2, k=0.1, r_p=0.01$).

effect of nanoparticles concentration on the velocity distribution. It is observed that the magnitude of the velocity decreases with different nanoparticle concentration, ϕ for $r_p \leq r \leq h(z)$. The results also produce the relationship between the amplitude ratio and the velocity $r_p \leq r \leq h(z)$.

For $r_p \leq r \leq h(z)$, the maximum velocity magnitude increases with amplitude ratio, δ for all parameters because of the increased pressure difference (ΔP) with amplitude ratio, as shown in Figure 4. One observes that the velocity decreases indefinitely also with increasing magnetic field, Ha for any given set of other parameters, see Figure 5.

Velocity profiles with different magnetic field

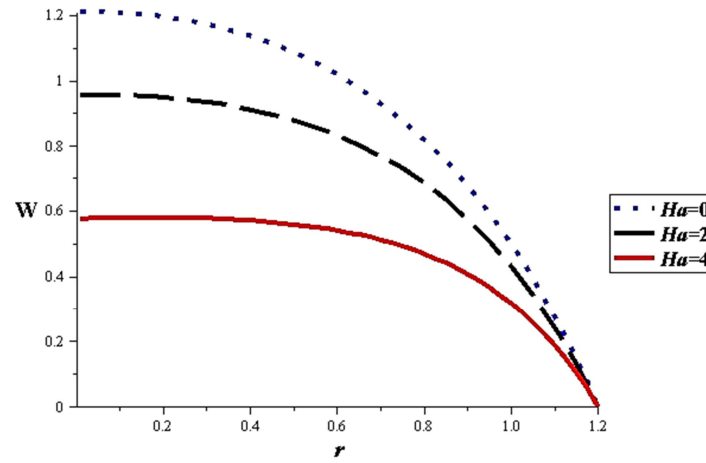


Figure 5. Velocity profiles with different magnetic field at ($A_1=1$, $A_2=0.01$, $A_3=1$, $\tau_y=0.05$, $\delta=0.2$, $\varphi=0.2$, $k=0.1$, $r_p=0.01$).

Velocity profiles with different porosity

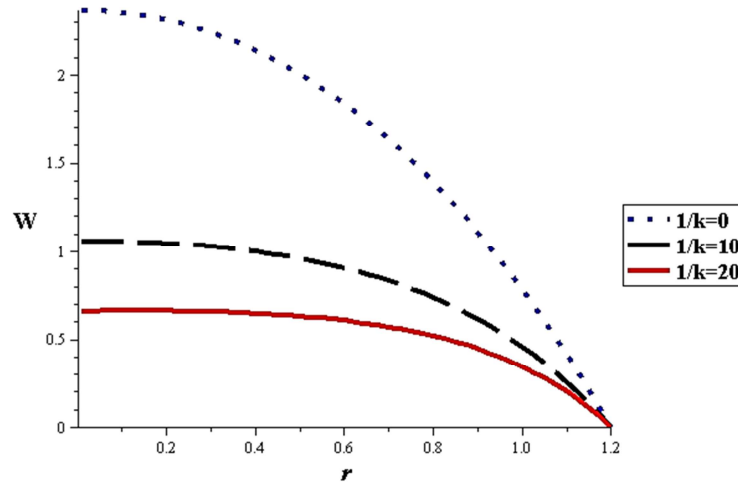


Figure 6. Velocity profiles with different porosity at ($A_1=1$, $A_2=0.01$, $A_3=1$, $\tau_y=0.05$, $\delta=0.2$, $\varphi=0.2$, $Ha=1.5$, $r_p=0.01$).

Velocity profiles with different wall damping (A_3)

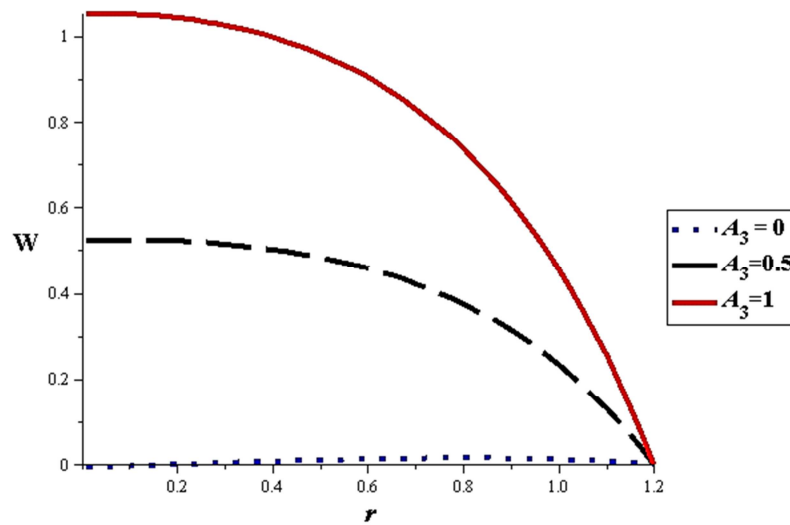


Figure 7. Velocity profiles with different wall damping (A_3) at ($A_1=1$, $A_2=0.01$, $k=0.1$, $\tau_y=0.05$, $\delta=0.2$, $\varphi=0.2$, $Ha=1.5$, $r_p=0.01$).

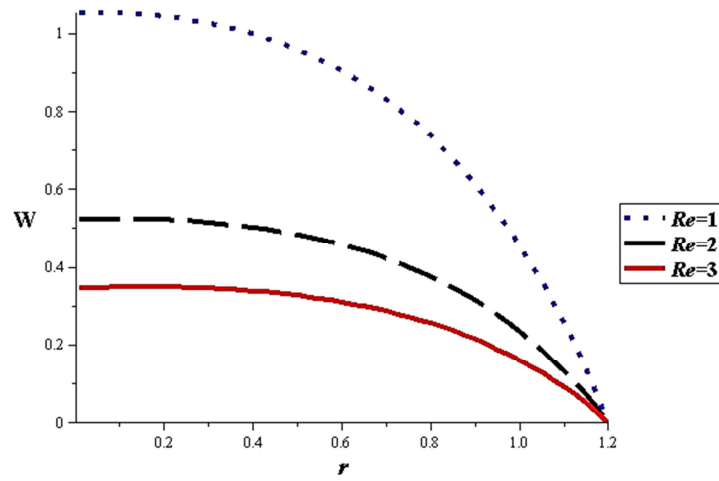
Velocity profiles with different Re 

Figure 8. Velocity profiles with different Re at $(A_1=1, A_2=0.01, A_3=1, k=0.1, \tau_y=0.05, \delta=0.2, \varphi=0.2, Ha=1.5, r_p=0.01)$.

Velocity profiles with different yield stress

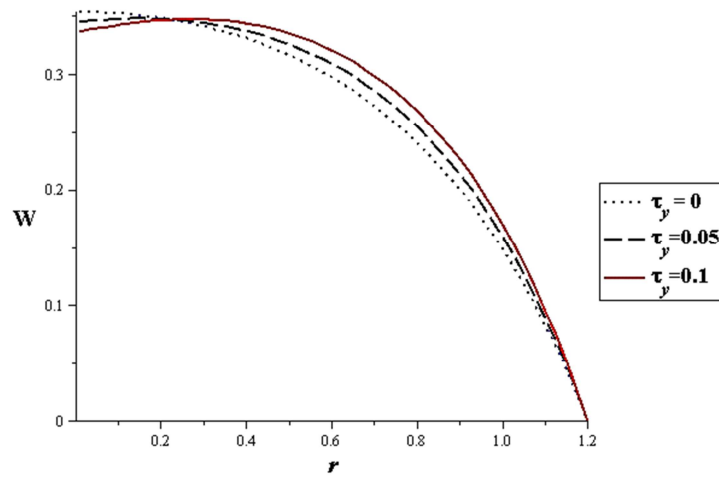


Figure 9. Velocity profiles with different yield stress at $(A_1=1, A_2=0.01, A_3=1, k=0.1, \delta=0.2, \varphi=0.2, Ha=1.5, r_p=0.01, Re=3)$.

Streamlines with nanoparticles concentration

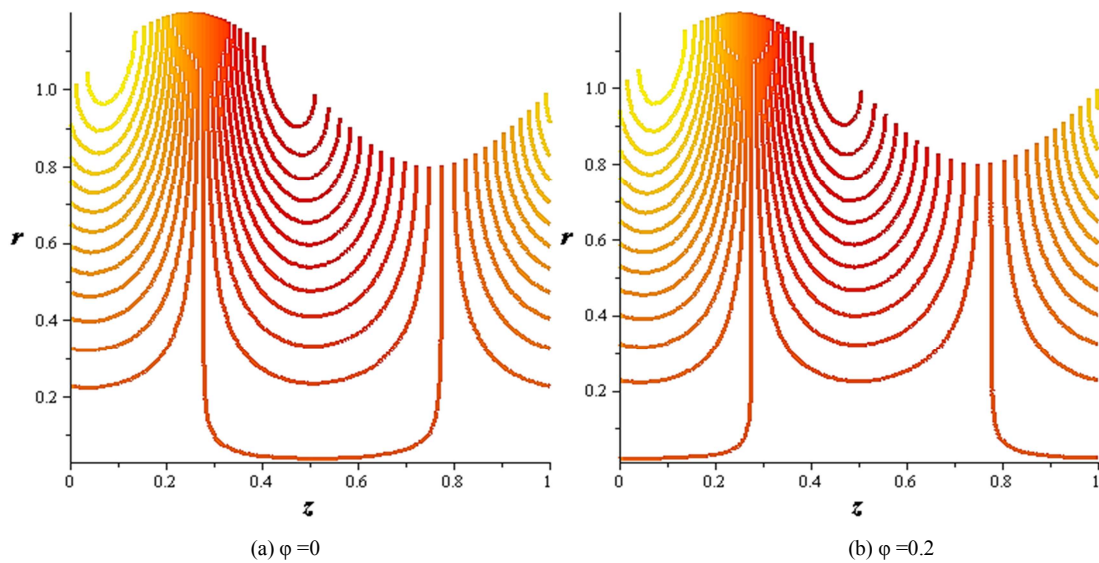


Figure 10. Streamlines with nanoparticles concentration at $(A_1=1, A_2=0.01, A_3=1, \tau_y=0.05, \delta=0.2, Ha=1.5, k=0.1, Re=1, r_p=0.01)$.

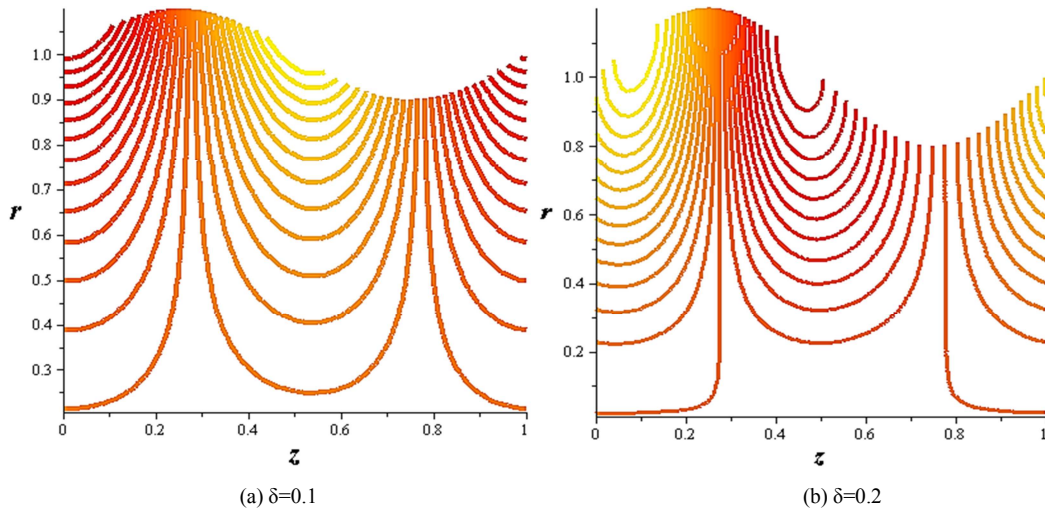
Streamlines with amplitude ratio

Figure 11. Streamlines with amplitude ratio at $(A_1=1, A_2=0.01, A_3=1, \tau_y=0.05, \varphi=0.2, Ha=1.5, k=0.1, r_p=0.01)$.

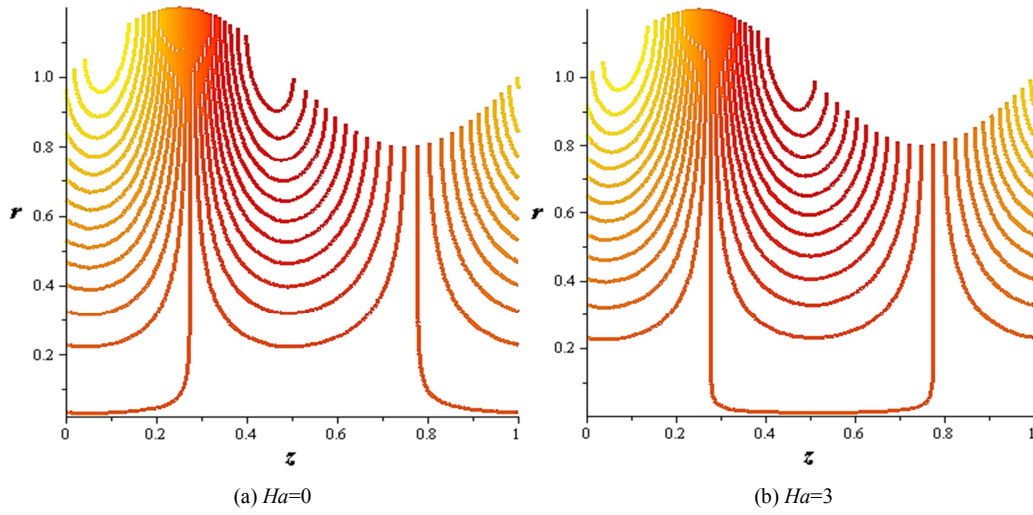
Streamlines with magnetic field

Figure 12. Streamlines with magnetic field at $(A_1=1, A_2=0.01, A_3=1, \tau_y=0.05, \delta=0.2, \varphi=0.2, k=0.1, r_p=0.01)$.

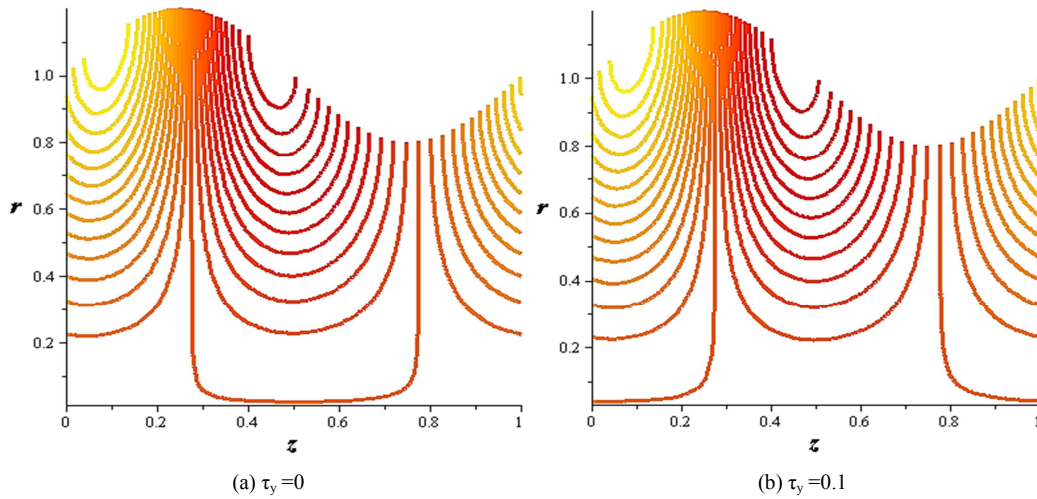
Streamlines with yield stress

Figure 13. Streamlines with yield stress at $(A_1=1, A_2=0.01, A_3=1, Ha=1.5, \delta=0.2, \varphi=0.2, k=0.1, r_p=0.01)$.

Pressure difference with different wall tension (A_1)

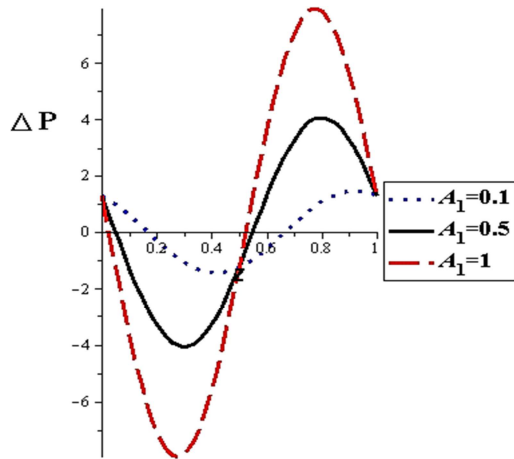


Figure 14. Pressure difference VS. Positions at different wall tension (A_1) at ($A_2=0.01$, $A_3=1$, $\delta=0.2$, $Re=1$).

Pressure difference with different wall damping (A_3)

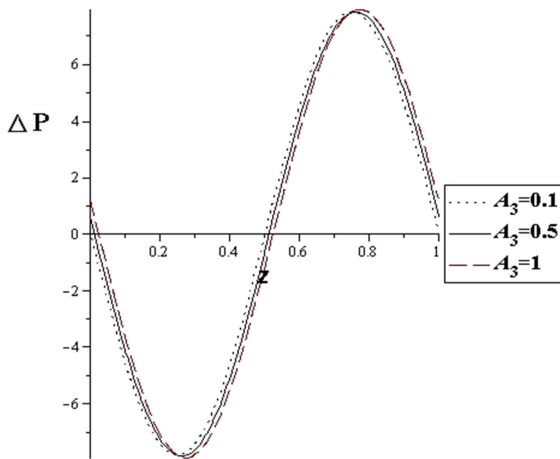


Figure 15. Pressure difference VS. Positions at different wall damping (A_3) at ($A_1=1$, $A_2=0.01$, $\delta=0.2$, $Re=1$).

Pressure difference with different amplitude ratio (δ)

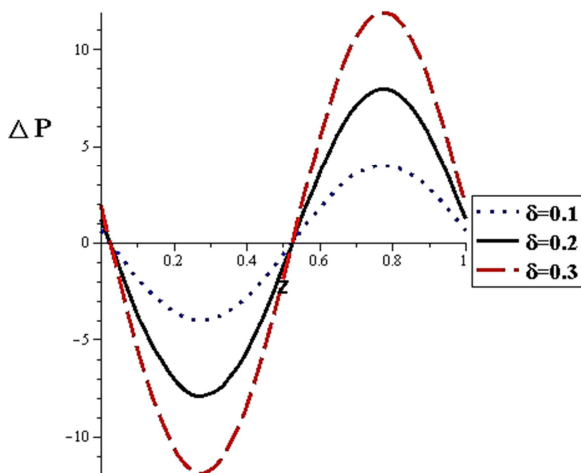


Figure 16. Pressure difference VS. Positions at different amplitude ratio (δ) at ($A_1=1$, $A_2=0.01$, $A_3=1$, $Re=1$).

Figure 6. represents the relation between the velocity profiles of the fluid with porous medium. It is observed that the permeability parameter (k) increases the velocity. With damping, the velocity increases, see Figure 7. It is observed that, Reynolds number decreases the flow velocity as shown in figure 8. Figure 9. show that the yield stress increases the velocity. Figure 10. shows the streamlines at different values of ϕ , while Figure 11. discusses the effects of amplitude ratio δ on the complicated behavior of streamlines. With increasing the magnetic field and the yield stress, the streamlines are strongly crowded; see Figure (12-13), while the nanoparticle concentration (ϕ) does not affect the streamlines.

The pressure difference along the artery affects the tension in the wall of artery, the damping of the wall and the amplitude ratio, where the wall tension or the amplitude ratio increases, pressure difference increases as shown in Figure (14-16). respectively. Figure 15. shows that there is small effect of wall damping on pressure difference.

4. Conclusion

In the present study, both effects of magnetic field and wall properties on a nanofluid with peristaltic transport in pipe are analyzed. An analytical solution of this problem under long-wavelength and low Reynolds number approximations is performed. Theoretical model to study the effects of nanoparticle concentration and the amplitude ratio on flow behavior in pipe is built up. The features of the flow characteristics are analyzed by plotting graphs and discussing them in detail. Results show that for a given nanoparticle concentration, the velocity increases with the amplitude ratio. The presence of magnetic field lead to decrease the flow velocity at any amplitude ratio. The effect of nanoparticles concentration, amplitude ration and magnetic field on the shape of streamlines have been studied. With increasing the magnetic field and amplitude ratio, the streamlines are strongly crowded, while the nanoparticle concentration (ϕ) does not affect the streamlines. The property of the wall plays a very vital role on the behavior of the flow such as the tension in the wall of human artery, the damping of the wall and the amplitude ratio. These parameters of the artery cause the pressure difference along the artery. It is noticed that the pressure difference increases because of the increasing of the wall tension. Wall damping of the artery wall is presented. There is small effect of wall damping on pressure difference.

Declarations

Author Contributions

Conceptualization. Islam Eldesoky and Ramzy Abumandour; methodology, Muhammad Magdy; software, validation, formal analysis, and investigation, Islam Eldesoky,

and Muhammad Magdy; resources, Muhammad Magdy; writing—original draft preparation, Muhammad Magdy; writing—review and editing. All authors have read and agreed to the published version of the manuscript.

ORCID

Muhammad Magdy: 0000-0002-4687-1675

Conflicts of Interest

The authors declare no conflicts of interest.

References

- [1] Kalbande, V. P., Vinchurkar, S., Nandanwar, Y. N., Verma, S. K., & Walke, P., "Global mathematical correlations for heat pipe and nanofluid based thermal energy storage system: Dimensional analysis approach," *Environmental Progress & Sustainable Energy*, e14285.
- [2] Kalbande, V. P., Walke, P. V., Untawale, S., & Mohan, M., "Performance Evaluation of Novel Heat Pipe-Assisted Thermal Storage System with Parabolic Trough Solar Collector Using Nanofluid," *Energy Technology*, 10, 9, 2022.
- [3] Kalbande, V. P., Walke, P. V., "Oil-and aluminum-based thermal storage system using flat plate solar collector," In *Smart Technologies for Energy, Environment and Sustainable Development: Select Proceedings of ICSTEESD*, 553-562, 2019.
- [4] Kalbande, Vednath P., Pramod V. Walke, and C. V. M. Kriplani, "Advancements in thermal energy storage system by applications of Nanofluid based solar collector," A review," *Environmental and Climate Technologies*, 24, 1, 310-340, 2020.
- [5] Kalbande, V. P., Walke, P. V., Rambhad, K., Mohan, M., & Sharma, A., "Performance enhancement of thermal energy storage systems using nanofluid. In *Energy Storage Systems, Optimization and Applications*, 135-149, 2022.
- [6] E. Mitsoulis, "Flows of viscoplastic materials: models and computations," *Rheology reviews*, vol. 2007, pp. 135-178, 2007.
- [7] N. Nirmalkar, R. Chhabra, and R. Poole, "On creeping flow of a Bingham plastic fluid past a square cylinder," *Journal of Non-Newtonian Fluid Mechanics*, vol. 171, pp. 17-30, 2012.
- [8] A. Bahadori, G. Zahedi, and S. Zendehboudi, "A novel analytical method predicts plug boundaries of Bingham plastic fluids for laminar flow through annulus," *The Canadian Journal of Chemical Engineering*, vol. 91, pp. 1590-1596, 2013.
- [9] M. Sayed-Ahmed, H. Saleh, and I. Hamdy, "Numerical Solution of the Extend Graetz Problem for a Bingham Plastic Fluid in Laminar Tube Flow," *Applied Mathematics*, vol. 3, pp. 27-37, 2013.
- [10] C. Picart, J.-M. Piau, H. Galliard, and P. Carpentier, "Human blood shear yield stress and its hematocrit dependence," *Journal of Rheology*, vol. 42, pp. 1-12, 1998.
- [11] S. Yadav and K. Kumar, "Bingham plastic characteristic of blood flow through a generalized atherosclerotic artery with multiple stenosis," *Advance in Applied Science Research*, vol. 3, pp. 3551-3557, 2012.
- [12] A. Singh and D. Singh, "A computational study of Bingham plastic flow of blood through an artery by multiple stenosis and post dilatation," *Advances in Applied Science Research*, vol. 3, pp. 3285-3290, 2012.
- [13] L. De Chant, "A perturbation model for the oscillatory flow of a Bingham plastic in rigid and periodically displaced tubes," *Journal of biomechanical engineering*, vol. 121, pp. 502-504, 1999.
- [14] J. Misra and G. Shit, "Blood flow through arteries in a pathological state: A theoretical study," *International Journal of Engineering Science*, vol. 44, pp. 662-671, 2006.
- [15] J. Misra and S. Maiti, "Peristaltic pumping of blood through small vessels of varying cross-section," *Journal of Applied Mechanics*, vol. 79, p. 061003, 2012.
- [16] J. Misra and A. Sinha, "Effect of thermal radiation on MHD flow of blood and heat transfer in a permeable capillary in stretching motion," *Heat and Mass Transfer*, vol. 49, pp. 617-628, 2013.
- [17] Kumar, Amit, Rajat Tripathi, and Ramayan Singh. "Von Kármán swirling flow and heat transfer analysis on MHD fluid subject to partial slip and temperature jump conditions," *Waves in Random and Complex Media*, 1-17, 2022.
- [18] Amit et al. "Unsteady mixed convective flow of hybrid nanofluid past a rotating sphere with heat generation/absorption: an impact of shape factor." *International Journal of Numerical Methods for Heat & Fluid Flow*, 2023.
- [19] Eldabe, N. T., G. M. Moatimid, and A. Sayed, "The effects of the pressure work and Hall currents in the MHD peristaltic flow of Bingham–Papanastasiou nanofluid through porous media," *Pramana* 95.2: 76, 2021.
- [20] Sultan, Faqiha, Najeeb Alam Khan, and Muhammad Idrees Afridi, "Investigation of biological mechanisms during flow of nano-Bingham–Papanastasiou fluid through a diseased curved artery," *Proceedings of the Institution of Mechanical Engineers, Part N: Journal of Nanomaterials, Nanoengineering and Nanosystems* 234, 3-4, 69: 81, 2020.
- [21] Basha, N. Z., Vajravelu, K., Mebarek-Oudina, F., Sarris, I., Vaidya, K., Prasad, K. V., & Rajashekhar, C., "MHD Carreau nanoliquid flow over a nonlinear stretching surface," *Heat Transfer*, 51, 6, 5262-5287, 2022.
- [22] Kumar, Ray, Saha, Tanwar, Kumar, Sheremet, "Flow of hybrid nanomaterial over a wedge: shape factor of nanoparticles impact," *The European Physical Journal Plus*, 138(10), 901, 2023.
- [23] Kumar, Amit, Rajendra K. Ray, and Mikhail A. Sheremet., "Entropy generation on double diffusive MHD slip flow of nanofluid over a rotating disk with nonlinear mixed convection and Arrhenius activation energy," *Indian Journal of Physics*, 1-17, 2022.
- [24] Ray, A. K., Vasu, B., Murthy, P. V. S. N., Anwar Bég, O., Gorla, R. S. R., & Kumar, B. "Convective flow of non-homogeneous fluid conveying nano-sized particles with non-Fourier thermal relaxation: application in polymer coating," *Arabian Journal for Science and Engineering*, 47(5), 6559-6576, 2022.

- [25] Vasu, B., Atul Kumar Ray, and Rama SR Gorla. "Free convective heat transfer in Jeffrey fluid with suspended nanoparticles and Cattaneo–Christov heat flux," *Proceedings of the Institution of Mechanical Engineers, Part N: Journal of Nanomaterials, Nanoengineering and Nanosystems*, 234. 3-4, 99-114, 2020.
- [26] Kumar, Amit, Ramayan Singh, and Mikhail A. Sheremet., "Analysis and modeling of magnetic dipole for the radiative flow of non - Newtonian nanomaterial with Arrhenius activation energy," *Mathematical Methods in the Applied Sciences*, 2021.
- [27] Ray, Atul Kumar, Rama Subba Reddy Gorla, and B. Vasu. "Homotopy simulation of non-Newtonian Spriggs fluid flow over a flat plate with oscillating motion," 2019.
- [28] Ray, Atul Kumar., "Novel numerical solution of non-linear heat transfer of nanofluid over a porous cylinder: Buongiorno-Forchheimer model," *Journal of Computational & Applied Research in Mechanical Engineering (JCARME)* 10.2, 485-496, 2021.
- [29] I. M. Eldesoky, "Slip effects on the unsteady MHD pulsatile Blood flow through porous medium in an artery under the effect of body acceleration," *International Journal of Mathematics and Mathematical Sciences*, vol. 2012, 2012.
- [30] S. R. Kumar, "Analysis of Heat Transfer on MHD Peristaltic Blood Flow with Porous Medium through Coaxial Vertical Tapered Asymmetric Channel with Radiation–Blood Flow Study," *International Journal of Bio-Science and Bio-Technology*, vol. 8, pp. 395-408, 2016.
- [31] M. El-Hakiem, "MHD oscillatory flow on free convection–radiation through a porous medium with constant suction velocity," *Journal of Magnetism and Magnetic Materials*, vol. 220, pp. 271-276, 2000.
- [32] K. S. Mekheimer, "Non-linear peristaltic transport of magnetohydrodynamic flow in an inclined planar channel," *Arabian Journal for Science and Engineering*, vol. 28, pp. 183-202, 2003.
- [33] T. Hayat and N. Ali, "Peristaltically induced motion of a MHD third grade fluid in a deformable tube," *Physica A: Statistical Mechanics and its applications*, vol. 370, pp. 225-239, 2006.
- [34] N. Ali, Q. Hussain, T. Hayat, and S. Asghar, "Slip effects on the peristaltic transport of MHD fluid with variable viscosity," *Physics Letters A*, vol. 372, pp. 1477-1489, 2008.
- [35] F. Abbasi, T. Hayat, A. Alsaedi, and B. Ahmed, "Soret and Dufour effects on peristaltic transport of MHD fluid with variable viscosity," *Applied Mathematics & Information Sciences*, vol. 8, p. 211, 2014.
- [36] S. R. Kumar, "Effect of Couple Stress Fluid Flow on Magnetohydrodynamic Peristaltic Blood Flow with Porous Medium through Inclined Channel in the Presence of Slip Effect-Blood Flow Model," *International Journal of Bio-Science and Bio-Technology*, vol. 7, pp. 65-84, 2015.
- [37] S. R. Kumar, "MHD Peristaltic Transportation of a Conducting Blood Flow with Porous Medium through Inclined Coaxial Vertical Channel," *International Journal of Bio-Science and Bio-Technology*, vol. 8, pp. 11-26, 2016.
- [38] I. Eldesoky, R. Abumandour, M. Kamel, and E. Abdelwahab, "The combined influences of heat transfer, compliant wall properties and slip conditions on the peristaltic flow through tube," *SN Applied Sciences*, vol. 1, no. 8, pp. 1-16, 2019.
- [39] J. Misra and S. Adhikary, "Flow of a Bingham fluid in a porous bed under the action of a magnetic field: Application to magneto-hemorheology," *Engineering science and technology, an international journal*, vol. 20, pp. 973-981, 2017.
- [40] Chu, W. K., and Fang, J., "Peristaltic transport in a slip flow", *The European Physical Journal B- Condensed Matter and Complex Systems*, 16(3): 543-547, 2000.
- [41] I. Eldesoky, R. Abumandour, M. Kamel, and E. Abdelwahab, "The combined effects of wall properties and space porosity on MHD two-phase peristaltic slip transport through planar channels," *International Journal of Applied and Computational Mathematics*, vol. 7, no. 2, pp. 1-37, 2021.
- [42] A. H. Shapiro, M. Y. Jaffrin, and S. L. Weinberg, "Peristaltic pumping with long wavelengths at low Reynolds number," *Journal of fluid mechanics*, vol. 37, pp. 799-825, 1969.